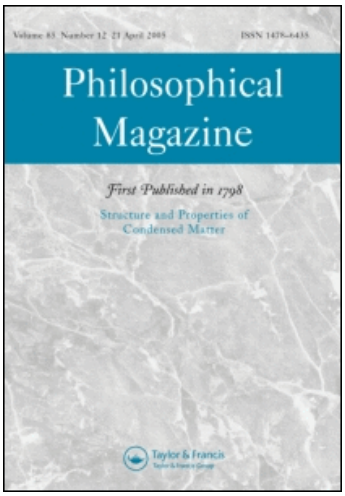

Philosophical Magazine
Publication details, including instructions for authors and subscription information:
http://www.informaworld.com/smpp/title~content=t713695589

Time domain response and the data analysis of ferroelectric discharge current

Lin Wu [a]; Xiaoyong Wei [a]; Shuangliang Di [b]; Xi Yao [a]
[a] Electronic Materials Research Laboratory, Key Laboratory of the Ministry of Education, Xi'an Jiaotong University, Xi'an 710049, China [b] Department of Mathematics, Xi'an Jiaotong University, Xi'an 710049, China

Online Publication Date: 01 May 2009

To cite this Article Wu, Lin, Wei, Xiaoyong, Di, Shuangliang and Yao, Xi(2009)'Time domain response and the data analysis of ferroelectric discharge current',Philosophical Magazine,89:15,1237 — 1250
To link to this Article: DOI: 10.1080/14786430902895770
URL: http://dx.doi.org/10.1080/14786430902895770

Philosophical Magazine
Vol. 89, No. 15, 21 May 2009, 1237–1250

Taylor & Francis
Taylor & Francis Group

Time domain response and the data analysis of ferroelectric discharge current

Lin Wu[a]*, Xiaoyong Wei[a], Shuangliang Di[b] and Xi Yao[a]

[a]*Electronic Materials Research Laboratory, Key Laboratory of the Ministry of Education, Xi'an Jiaotong University, Xi'an 710049, China;*
[b]*Department of Mathematics, Xi'an Jiaotong University, Xi'an 710049, China*

(*Received 4 October 2008; final version received 3 March 2009*)

The time domain method is more reliable for the study of nonlinear dielectric response compared with frequency domain analysis. A Tikhonov regularization method, which is widely adopted for ill-posed problem, is described for derivation of the relaxation time distribution function, $g(\tau)$, from the ferroelectric discharge current in time domain. The new method allows study of the structure variation and the relaxation behavior of ferroelectrics at different temperatures. For barium stannate titanate ceramics (BTS20), $g(\tau)$ has been successfully derived; the relaxation peaks move to shorter times with increasing temperature in the range 20–60°C, which may indicate a space charge thermal activation process. However, $g(\tau)$ could not be derived from the discharge current by the regularization method for BTS20 at temperatures above 60°C or for lanthanum-doped lead zirconium titanate transparent ceramic (PLZT), since the data do not satisfy the discrete Picard condition, which is a valid criterion for regularization method.

Keywords: time domain response; ferroelectrics; relaxation time; distribution function; ill-posed problem; Tikhonov regularization

1. Introduction

As a special group of polar crystals, much attention has been paid to ferroelectrics characterized by the fact that the polarization can be redirected by external electric fields. However, only little is known about the types and the dynamics of structure variation inside a ferroelectric ceramic under an external electric field.

The method of studying the relationship between physical variables and time in an external electric field is called the time domain method, which is different from the frequency domain method usually used in the study of ferroelectrics dielectric properties. The time domain method can reflect directly the dielectric response for stepwise, impulse or arbitrary external electric field. In addition, it is possible

*Corresponding author. Email: ferrum_gen@sina.com.

ISSN 1478–6435 print/ISSN 1478–6443 online

DOI: 10.1080/14786430902895770
http://www.informaworld.com

to derive the relaxation time distribution function, $g(\tau)$, which is the eigenfunction of dielectric relaxation, from the time domain response. Most importantly, the distribution function can provide information directly for understanding the processes of ferroelectric structure variation.

Long time scale (up to 10^4 s) dielectric responses, which contain information about slow processes, such as space charge injection, transportation, etc, can usually be described by the universal relaxation law (URL) proposed by Jonscher [1,2]. Differing from the simplified ideal Debye model, the URL is characterized by a fractional power law in both time and frequency domains. Debye relaxation corresponds to a single relaxation time, τ, whereas the URL may correspond to a series of relaxation times, or relaxation time distribution, $g(\tau)$. Although much work has been reported on the time domain response for dielectrics [3–6], reports about deriving the relaxation time distribution spectrum by the time domain method are still absent. The differential time domain spectrum method used by Li [7] was only able to indicate separated multi-relaxation times.

As is known, the relaxation function $f(t)$, which is proportional to the discharge current, can be derived directly from the current density. Current density data can be obtained by application of a stepwise electric field to a sample and then removal of external electric field. According to the equation $f(t) = A\int_0^\infty \frac{1}{\tau} g(\tau)\exp(-t/\tau)\mathrm{d}\tau$ [8], $g(\tau)$ can be calculated via the inverse Laplace transformation of $f(t)$. Experimentally, the current data is discrete, thus the integration corresponds to linear equations $Ax = b$. Unfortunately, the equations are an ill-posed problem and cannot be resolved by the ordinary least squares method. Tikhonov regularization [9], which is a data algorithm usually used in inverse problems such as analyzing the echo of an electromagnetic wave and reconstructing the blurred image, was employed to obtain $g(\tau)$. Similar work was performed by Banys [10], where Tikhonov regularization was used in resolving $g(\tau)$ from frequency domain data on complex dielectric constant data of $(Sr,Ba)Nb_2O_6$.

This paper aims at deriving $g(\tau)$ from the ferroelectric discharge current in the time domain. The samples considered are relaxor ferroelectric barium stannate titanate ceramics (BTS20) and lanthanum-doped lead zirconium titanate transparent ceramics (PLZT). The experiment and data processing procedures are interesting, and we attempt to find a new way of characterizing the dynamic behaviors of ferroelectric structure variation.

2. Experiment

As shown in Figure 1, the experimental system contains a Keithley 6485 picoammeter, a SRS PS350 5000V high-voltage source, a home-made constant temperature system and a computer for data recording.

Samples were placed in a constant temperature system at temperatures in the range of 30–160°C. A 100 V electric voltage was applied to the sample for more than 60 min to ensure sufficient charging, and then the external electric field was removed. Under a short-circuit condition (switch to position a), the picoammeter measures the discharge current and a computer program collects the current data at intervals of 1–2 s through the GPIB interface of the picoammeter.

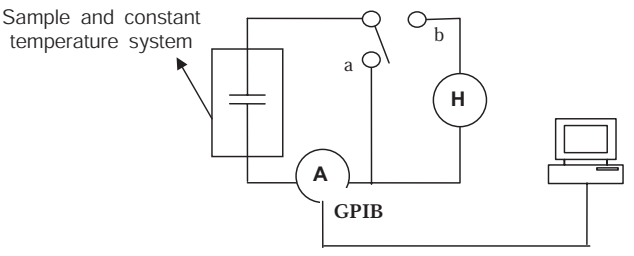

Figure 1. Current measurement setup: H = high-voltage source; A = picoammeter.

3. The principle of data analysis

3.1. *The relationship between current, j(t), and g(τ)*

As is known, the discharge current density is a differentiate of polarization with respect to the time of a relaxation process, $j(t) = \frac{dP_r}{dt} = (\varepsilon_s - \varepsilon_\infty)\varepsilon_0 E_0 f(t)$, where $j(t)$ is the discharge current density derived from experiment, P_r is the relaxational polarization and $f(t)$ is the relaxation function.

If there is a single relaxation time in the dielectric, where $g(\tau)$ is a δ function, the relaxation function is as follows: $f(t) = \frac{1}{\tau}\exp(-t/\tau)$. Otherwise, if there is distribution of relaxation times in the dielectric, the relaxation function is $f(t) = B\int_0^\infty \frac{1}{\tau}\exp(-t/\tau)g(\tau)d\tau$; therefore,

$$j(t) \propto f(t) = B\int_0^\infty g(\tau)\frac{1}{\tau}\exp(-t/\tau)d\tau, \tag{1}$$

where $g(\tau)$ is the distribution function of relaxation times, which is the goal to be derived from Equation (1). The above integral equation can be replaced with discrete linear equations in realistic problems,

$$Ax = b, \tag{2}$$

where $A = \frac{1}{\tau}\exp(-t/\tau)$, $x = g(\tau)$ and $b = j(t)$. By solving the equations $Ax = b$ with the least squares method as usual, we find immediately that we obtain completely different answers even if the discharge current data contain negligible errors, which indicates mathematical difficulties! The difficulty comes from the fact that the equation is an ill-posed problem, which must be solved by a regularization method [11]. We are going to adopt Tikhonov regularization method, described in the appendix I, to calculate the distribution function $g(\tau)$ from time domain current data.

3.2. *Mathematical criterion*

There is a most important criterion, the discrete Picard condition (DPC), in the Tikhonov regularization. If DPC is satisfied, the resolution is reasonable. Otherwise it means nothing. After obtaining the discharge current data, the first thing we should do is to check whether DPC is satisfied, which means whether we can find a suitable solution for Equations (1) and (2).

The singular value decomposition (SVD) of matrix **A** is a decomposition of the form: $\mathbf{A} = U\sum V^T = \sum_{i=1}^n u_i\sigma_i v_i^T$, where $U = (u_1, \ldots u_n)$ and $v = (v_1, \ldots v_n)$ are

matrices with orthonormal columns, $U^TU = V^TV = I_n$ and where $\sum = \mathrm{diag}(\sigma_1, \ldots, \sigma_n)$ has non-negative diagonal elements appearing in non-increasing order.

If the SVD of matrix **A** is used in the least squares method, then we can obtain the least squares solution:

$$x_{LS} = \sum_{i=1}^{n} \frac{u_i^T b}{\sigma_i} v_i. \tag{3}$$

For an ill-posed problem, the singular values, σ_i, of **A** decay gradually toward nearly zero and the condition number of **A** ($\mathrm{cond}(\mathbf{A}) = \sigma_1/\sigma_n$) is very large. The condition about solvability of Equations (3) is whether the convergence rate of $|u_i^T b|$ is faster than the convergence rate of σ_i. The criterion DPC refers to whether the Fourier coefficients $|u_i^T b|$ of the unperturbed right-hand side of Equation (2) decay to zero faster than the singular values σ_i do [12]. If $|u_i^T b|$ decay faster than σ_i, DPC is satisfied. So, DPC is actually a criterion for solvability of the equations.

A Picard plot (generated by using the routine 'Picard' in Regularization Tools [9]) enables a visual check of the discrete Picard condition. A Picard plot shows the variation of σ_i, $|u_i^T b|$ and $|u_i^T b|/\sigma_i$.

In practice, the experimental data right-hand side of Equation (2) are usually contaminated by measurement errors, approximation errors, and so on. So the given perturbed problem rarely satisfies the DPC. However, if the underlying exact problem satisfies the DPC, we may see that Fourier coefficients $|u_i^T b|$ still decay faster than the singular values σ_i above the level of noise. In this case, we can say that the problem satisfies the DPC (see Figure 2). The two plots in Figure 2 correspond to two different noise levels: 10^{-5} and10^{-3}. The $|u_i^T b|$ value level off at 10^{-5} and 10^{-3}, which are the noise levels. The larger the noise, the fewer terms, $|u_i^T b|$, remain above the noise level and can be trusted. The essence of a regularization method is to keep those components (for small indexes i), $|u_i^T b|/\sigma_i$, and preferably dampen the components, $|u_i^T b|/\sigma_i$, which are dominated by the noise ($|u_i^T b|$ level off noise) by multiplying it with a filter factor less than unity. More details of the Tikhonov regularization method can be found in the appendix. Mathematically, it is realized by

$$x_\lambda = \sum_{i=1}^{n} f_i \frac{|u_i^T b|}{\sigma_i} v_i, \tag{4}$$

where the scalars f_i are referred to as the filter factors.

DPC is a necessary condition for obtaining acceptable regularized solution. The reasons that a problem does not satisfy DPC are probably: the error in right-hand side of Equation (2) is too large; insufficient collected data (right-hand side of Equation (2)) for meaningful analysis; physical relation of the underlying exact problem is not reasonable.

4. Experimental results and data processing

A 100 V voltage was applied to PLZT and BTS20 samples for 60 min at different constant temperatures in the range 30–200°C. About 3000 discharge current data

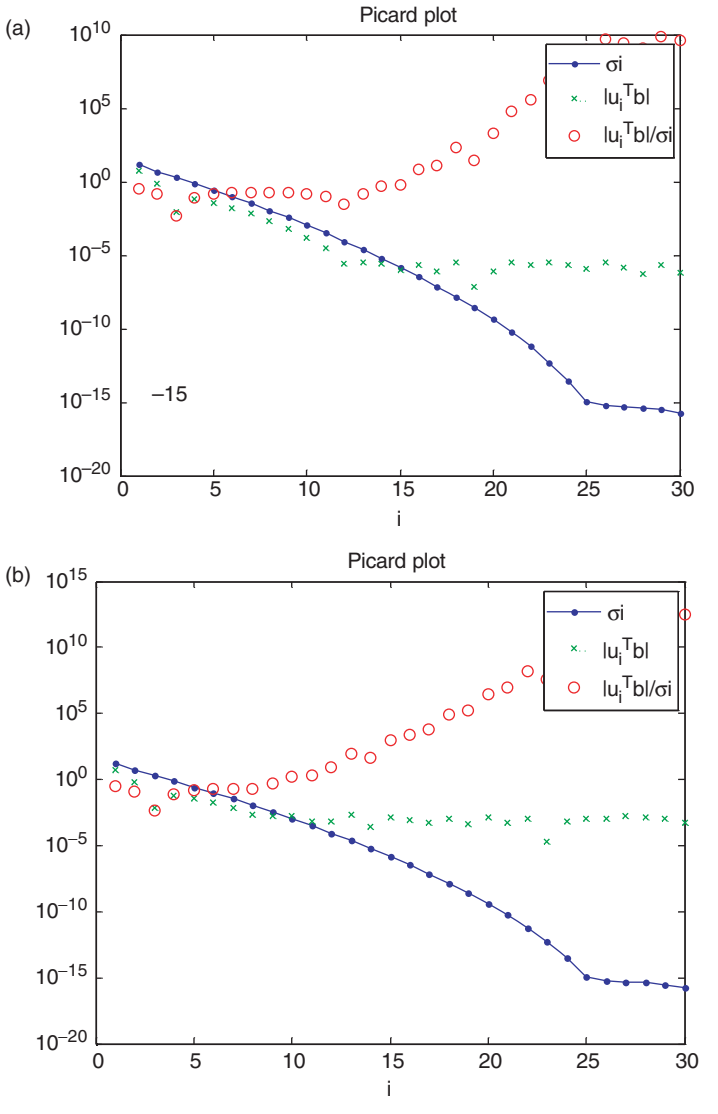

Figure 2. (Color online). The Picard plots for an ill-posed problem with noise: (a) noise level 10^{-5}; (b) noise level 10^{-3}.

points were collected in 60 min at each temperature. Time spectra of the discharge currents of PLZT and BTS20 samples are different in log–log plots (see Figures 3–4).

PLZT discharge current–time spectra exhibit a linear relationship in log–log current–time coordinates, which obey the URL [1,2] advanced by Jonscher (see Figure 3). They can be roughly described by the power law: $I = At^{-n}$.

The fitted exponents n are listed in Table 1. These values are larger than unity, corresponding to $m+1$ [1, 2]; therefore, the values of m are in the range 0.14–0.21, as listed in Table 1.

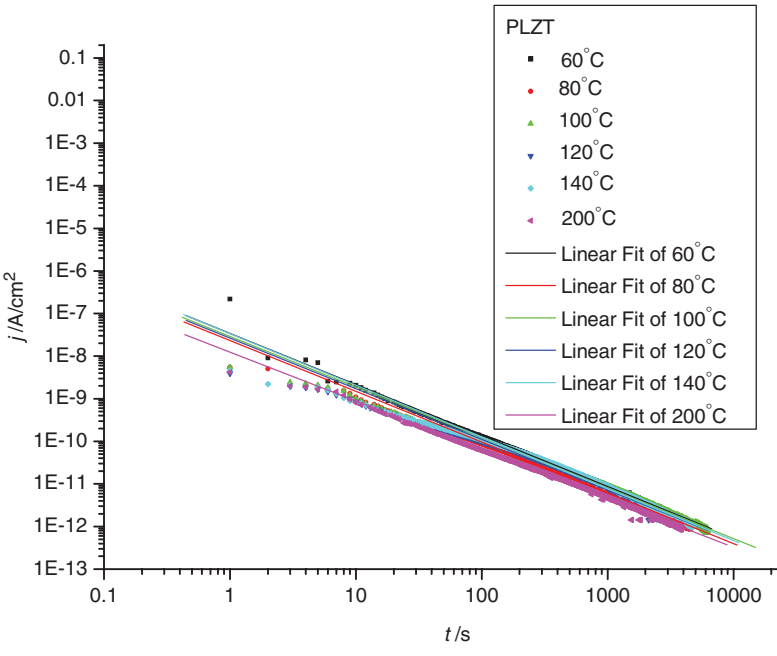

Figure 3. (Color online). Discharge current of PLZT in the range 60–200°C (voltage 100 V, sample thickness 1 mm).

Discharge current–time spectra of BTS20 at different temperatures are shown in Figure 4. Comparing with the spectra for PLZT, the two current curves are quite different. They are similar to an exponent function, which obeys the near-Debye relaxation at low temperature (30–60°C), and are neither linear nor obey an exponent function in log–log coordinates at higher temperature (60–90°C).

The Tikhonov regularization method was used to derive the distribution function of relaxation times, $g(\tau)$, from discharge current data. For comparison, the differential time domain spectrum method was also used. Calculating the derivative of product of current and time is referred to as the differential time domain spectrum method. The peaks correspond to separate relaxation times [7]. Using the Tikhonov regularization method, we intend to find the distribution profile of relaxation times, whereas the differential time domain spectrum method is used to locate the separated relaxation times.

4.1. $g(\tau)$ *of BTS20*

4.1.1. *At 30–60°C*

100 points of τ are equally spaced in logarithm range of 1–4000 s, because the current data is in the range 1–4000 s. Establish equations in 4000 variables:

$$\sum_{i=1}^{4000}\sum_{j=1}^{100}\frac{1}{\tau_j}\exp(-t_i/\tau_j)g(\tau_j) = I. \tag{5}$$

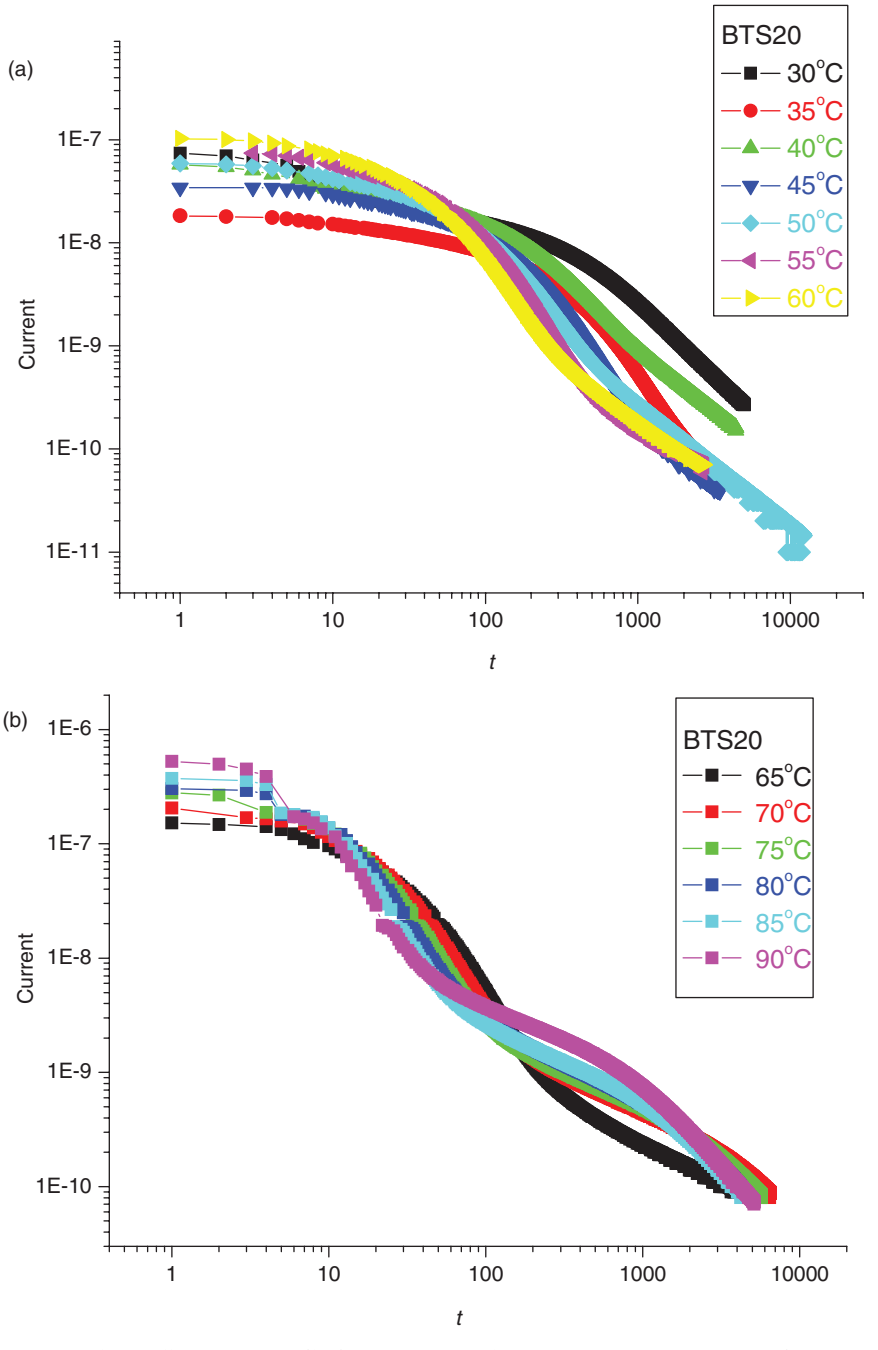

Figure 4. (Color online). BTS20 discharge current time spectrum (a) 30–60°C; (b) 60–90°C.

Table 1. Exponent n at different temperatures.

Temperature	60°C	80°C	100°C	120°C	140°C	200°C
n	1.19807	1.19143	1.18558	1.18909	1.21398	1.14433
$m=n-1$	0.19807	0.19143	0.18558	0.18909	0.21398	0.14433

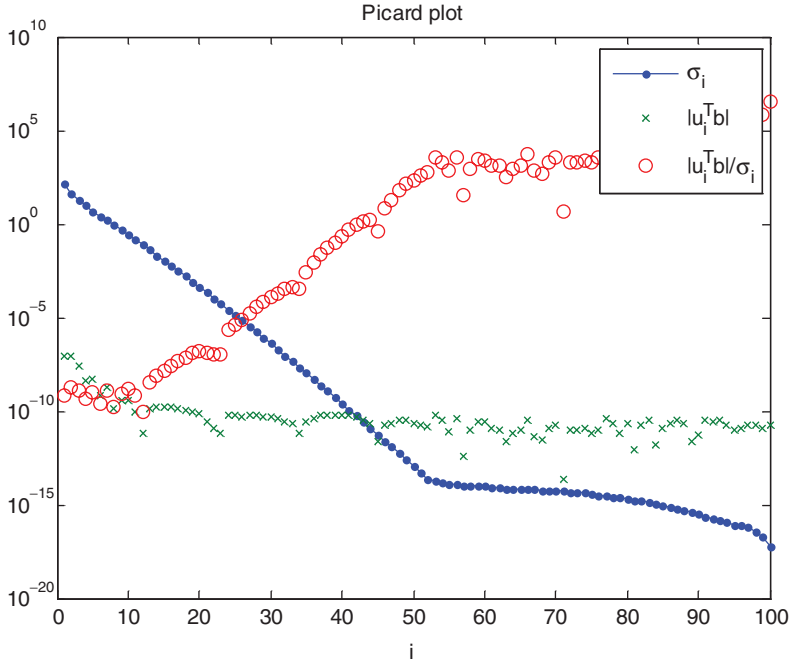

Figure 5. Picard plot of BTS20 at $T=35$°C. $|u_i^T b|$ decays faster than the singular values σ_i above the noise level 10^{-10}, which indicates that Equations (5) satisfy the DPC, and a proper solution can be found.

The coefficients, $\sum_{i=1}^{4000}\sum_{j=1}^{100}\frac{1}{\tau_j}\exp(-t_i/\tau_j)$, are decomposed by SVD and the Picard plot is obtained (see Figure 5). It can be seen that the noise is about 10^{-10} and the terms $|u_i^T b|$ also level off at 10^{-10}. $|u_i^T b|$ values decay faster than the singular values σ_i above the noise level 10^{-10}, which indicates that Equation (5) satisfies the DPC. This enables us to find a proper solution from these ill-posed equations by the Tikhonov regularization method. The results are shown in Figure 6.

Two separate peaks are shown in Figure 6. The first peak is less meaningful because of the unstable start of the current data. However, we pay close attention to the second peak, which moves toward shorter times with increasing temperature. At the same time, differential time domain spectrum method is used to verify the position of peaks (see Figure 7) and the results are shown in Table 2. The peaks obtained by both methods are close to each other for different temperatures.

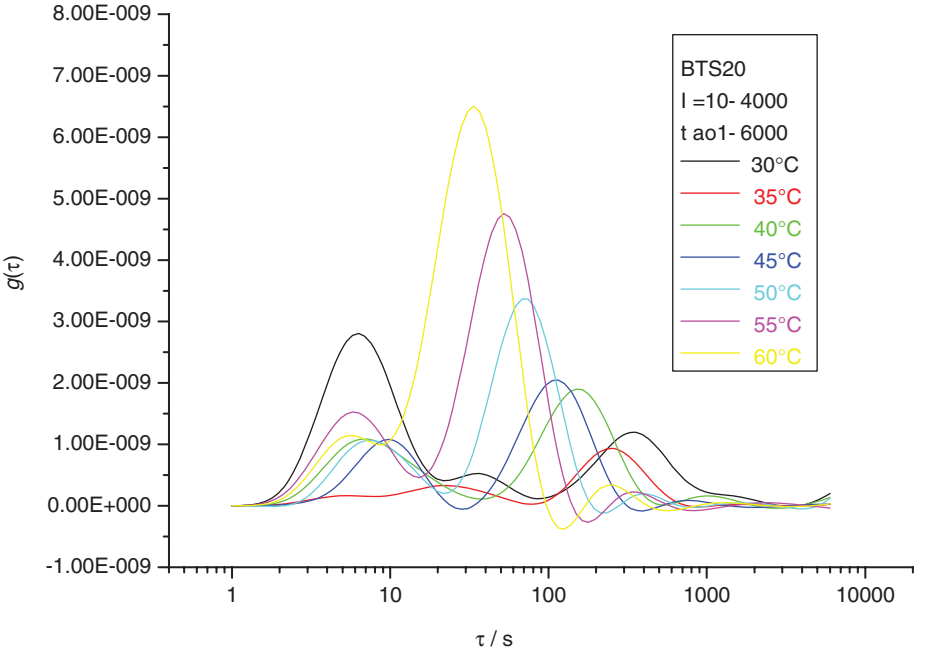

Figure 6. (Color online). $g(\tau)$ of BTS20 in the temperature range from 20°C to 60°C. The first peak is less meaningful because of the unstable start of current data. We pay attention to the second peak, which moves toward shorter times with increasing temperature.

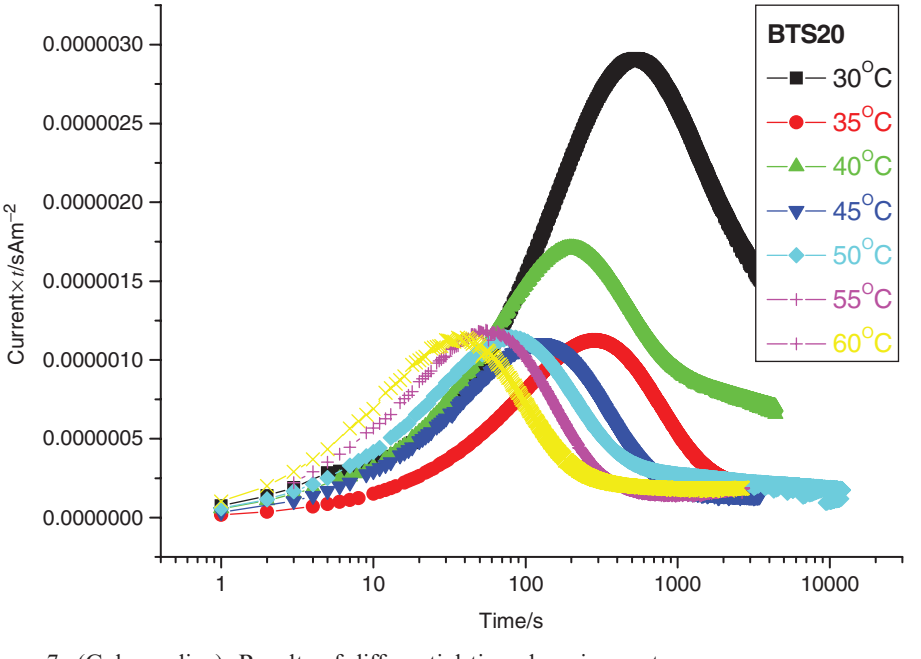

Figure 7. (Color online). Results of differential time domain spectrum.

Table 2. Comparation of Tikhonov method with differential time domain spectrum method.

Temperature (°C)	30	35	40	45	50	55	60
Tikhonov regularization method	360	250	160	115	80	52	33
Differential time domain method	520	270	190	120	80	55	35

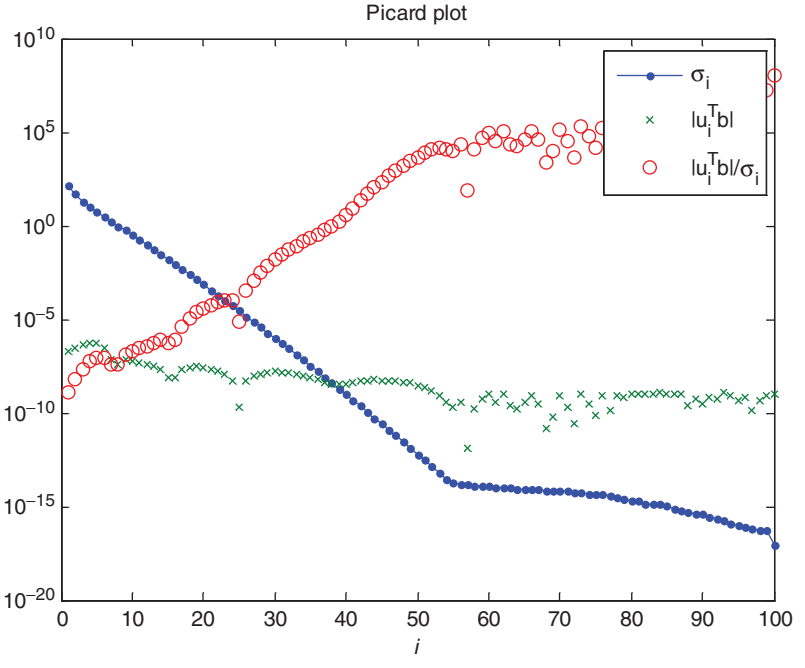

Figure 8. (Color online). Picard plot for BTS20 at $T = 90°C$. $|u_i^T b|$ always decays slower than σ_i, so DPC cannot be satisfied and there is no reasonable regularization solution to Equation (5).

4.1.2. *At 60–120°C*

When the temperatures are higher than 60°C, the discharge current–time spectra obey neither linear nor exponent functions (see Figure 4). A Picard plot shows that DPC cannot be satisfied even for the first current data (see Figure 8), which indicates that there is no reasonable regularization solution to Equations (5).

4.2. *g(τ) of PLZT*

The discharge current–time spectra of PLZT are in the form of a power function, obeying the URL (see Figure 3). However, a Picard plot shows that it does not satisfy the DPC (see Figure 9). As mentioned before, DPC is a necessary condition for obtaining reasonable regularized solution. Therefore, we can not find a regularization solution for PLZT, as for BTS20 at temperatures higher than 60°C.

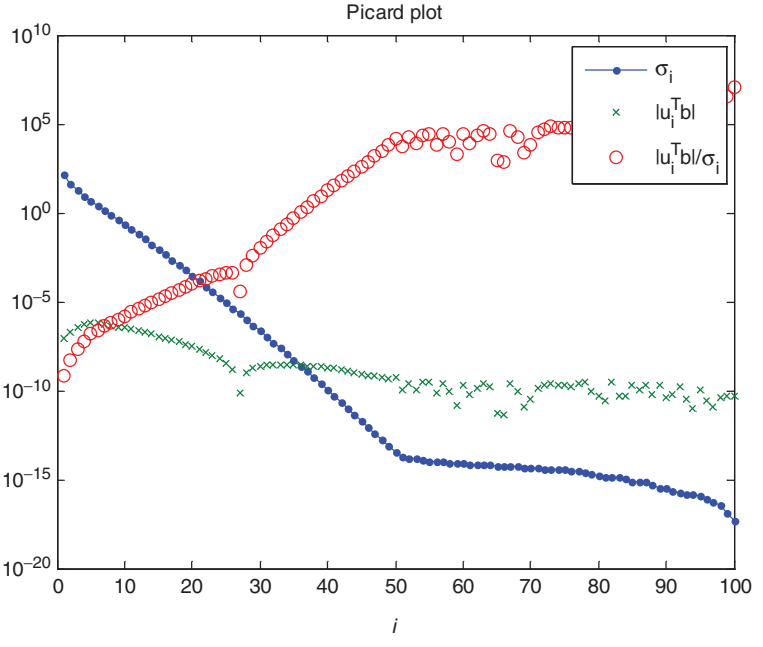

Figure 9. (Color online). Picard plot for PLZT at $T = 60^{\circ}$C; it does not satisfy the DPC.

5. Discussion

The distribution function, $g(\tau)$, can be derived from Equation (1) for near-Debye dielectric relaxation, such as in the case of BTS20 at temperatures 30–60°C, for which the discharge current–time spectrum is approximated to an exponent function. The curve of $g(\tau)$ reveals the regularity with which the peak position of the relaxation time moves toward shorter times, from 350 s to 30 s, with increasing temperature and the peak position is closely matched with the results derived by the differential time domain spectrum method.

In particular, the relaxation time at room temperature is comparable to the relaxation time results obtained previously by the present authors [13,14]. The experiment of slow relaxation of piezoelectric resonance shows that this relaxation is related to the injection and transportation of space charge [13,14]. The thermal activation behavior of space charge relaxation may be obtained from relaxation current spectrum at different temperature. This is interesting for us. Furthermore, the profiles of $g(\tau)$ at different temperatures may contain much more unknown information related to structure variations inside ferroelectrics.

For BTS20 at temperatures above 60°C and PLZT, $g(\tau)$ can not be derived from Equation (1) by the Tikhonov regularization method. As mentioned above, data error, the lack of data and improper relationship of Equation (1) may lead to this situation. Excluding data error, we propose that the reason $g(\tau)$ cannot be derived from Equation (1) both for BTS20 above 60°C and for PLZT is either the lack of data or Equation (1) is inapplicable. It is clear that a monotonically increasing current curve can not be described by Equation (1) at all. Considering the two joint

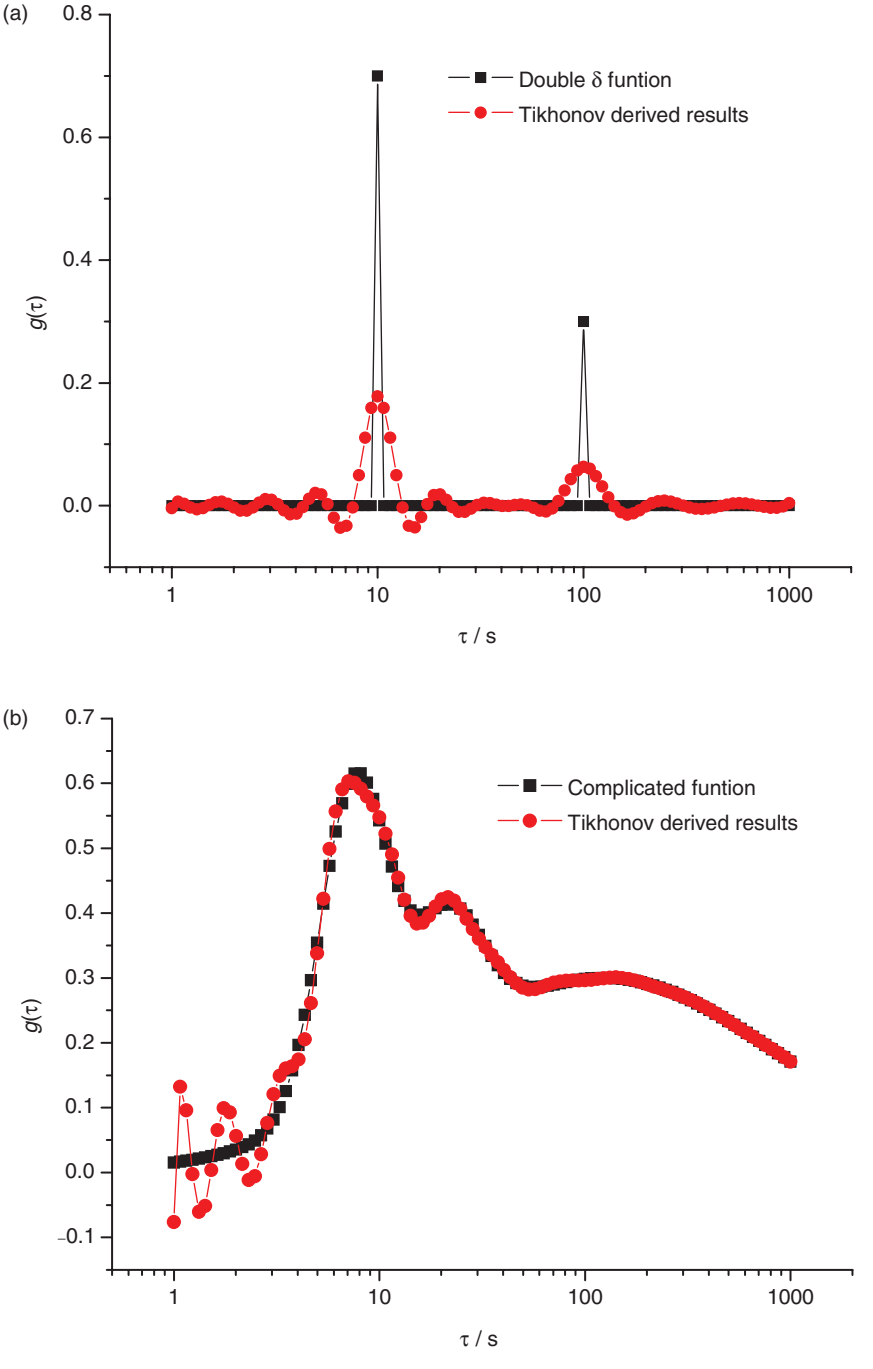

Figure 10. (Color online). The squares are $g(\tau)$, which we have set, and the circles are the $g(\tau)$ results that we derived by the Tikhonov regularization method: (a) $g(\tau)$ set as a double δ function; (b) $g(\tau)$ set as a complicated function.

lines behavior in time domain response of URL (for example, for PLZT) presented by Jonscher [1,2] the difficulty may come from the limitation of experiment conditions; in other words, the difficulty may be solved if a wider range of current data is collected.

6. Conclusion

The distribution function of relaxation times, $g(\tau)$, can be derived from BTS20 discharge current at 20–60°C by the Tikhonov regularization method. The peak position of the relaxation time moves to shorter times with increasing temperature, which indicates a thermally activation process of space charge relaxation. In both cases, for BTS20 at temperatures above 60°C and PLZT, $g(\tau)$ can not be derived from Equations (5) by the regularization method because of inadequate experiment conditions (the lack of data) or improper application of Equation (5).

Acknowledgements

This work was supported by the Ministry of Sciences and Technology of China through 973-project under grant No. 2002CB613304 and project 50402015 supported by the National Natural Science Foundation (NSFC) of China and the NCET program. The work was also supported by NSFC under grant No. 50872107.

References

[1] A.K. Jonscher, *Dielectric Relaxation in Solids*, Chelsea Dielectrics Press, London, 1983.
[2] A.K. Jonscher, *Universal Relaxation Law*, Chelsea Dielectrics Press, London, 1996.
[3] W.J. Merz, Phys. Rev. 95 (1954) p.690.
[4] Y. Ishibashi and I. Takagi, Jpn. J. Phys. Soc. 31 (1971) p.506.
[5] V. Shur, E. Rumyantsev and S. Makarov, J. Appl. Phys. 84 (1998) p.445.
[6] L. Jin, X. Yao, X.Y. Wei and Z.Z. Xi, Appl. Phys. Lett. 87 (2005) p.072910.
[7] J.D. Li, *Theory of Dielectrics*, Science Publishing House, Beijing, 2003.
[8] C.J.F. Bōttcher and P. Bordewijk, *Theory of Electric Polarization*, 2nd ed., Vol. 2, Elsevier, Amsterdam, 1978.
[9] P.C. Hansen, software available at http://www.imm.dtu.dk/~pch
[10] J. Banys, J. Macutkevic, R. Grigalaitis and W. Kleemann, Phys. Rev. B 72 (2005) p.024106.
[11] P.C. Hansen, *Rank-Deficient and Discrete Ill-Posed Problems: Numerical Aspects of Linear Inversion*, SIAM, Philadelphia, 1998.
[12] P.C. Hansen, BIT 30 (1990) p.658.
[13] X.Y. Wei, L. Jin and X. Yao, Appl. Phys. Lett. 87 (2005) p.082905.
[14] X.Y. Wei, Y.J. Feng and X. Yao, Appl. Phys. Lett. 84 (2004) p.1534.

Appendix 1. Tikhonov regularization method

Tikhonov regularization method

The form of Tikhonov regularization method used in this paper is

$$x_\lambda = \min_x \{\|Ax - b\|^2 + \lambda^2 \|x\|^2\}, \quad A \in R^{m \times n},\ m \geq n,\ b \in R^m. \tag{6}$$

With respect to lease squares method, an additional regularization term is added to the minimum. The role of this regularization term is to ensure that the norm of the solution should be lower than that of the lease square solution, which would become abnormally large at some point. Choosing proper λ to make a compromise between minimization of $\|Ax - b\|^2$ and $\|x\|^2$ is important. The assistant tool for choosing proper λ is L-Curve [9].

Using the SVD, the solution of the Tikhonov regularization method given by Equation (6) is given by $x_\lambda = \sum_{i=1}^{n} \frac{\sigma_i^2}{\sigma_i^2=\lambda^2} \frac{u_i^T b}{\sigma_i} v_i$, where the filter factor $f_i = \frac{\sigma_i^2}{\sigma_i^2+\lambda^2}$, An important property of the filter factor is that as σ_i decrease the corresponding f_i tend to zero. When $\lambda \to 0$, and $x_\lambda \to x_{LS}$, different f_i selection leads to a different regularization method. In the present paper, the Tikhonov regularization method is used.

Validity check of Tikhonov regularization method

We generate a discharge current data set from Equation (1), in which $g(\tau)$ are known, and then derive $g(\tau)$ from the supposed discharge current data in the reverse direction by the Tikhonov regularization method. The result should fit with the original $g(\tau)$, which is known. We perform these two steps to check the validity of the algorithm.

In Figure 10, the squares are $g(\tau)$, which we have set, including a double δ function and a complicated function. The circles are the results that we have derived for $g(\tau)$ by the Tikhonov regularization method. These figures illustrate that the Tikhonov regularization method can derive $g(\tau)$ correctly.